Interfacial Phases and Defects Characteristics of Al/Cu-Zn Bimetal Produced Via Centrifugal Casting Process

M. Gholami and M. Divandari *

* *divandari@iust.ac.ir*

Received: January 2018 Accepted: August 2018

School of Metallurgy and Materials Engineering, Iran University of Science and technology (IUST), Tehran, Iran.
DOI: 10.22068/ijmse.15.2.

Abstract: *Centrifugal casting process, in both horizontal and vertical mode, is considered as an efficient method to produce bimetallic components. Al/Cu65Zn35 couples were prepared by the vertical centrifugal casting process. In this study, different volume of molten aluminum having melt-to-solid (m/s) volume ratios (VR) of 1.5 and 2.5, were cast into preheated brass bush rotating at 800, 1600, and 2000 (rpm), respectively. The thickness of the interface, which is composed of three different zones, is depended on the rotational speed and the (VR) and was at least 490µm (at VR= 1.5 and 2000 rpm) and at most 1480 µm (at VR= 2.5 and 800 rpm). The results of optical microscopy, energy dispersive X-ray spectroscopy (EDS), and X-ray diffraction analysis showed that the interface layers are composed of Al2Cu5Zn4, Al3Cu3Zn, Al2Cu precipitates dispersed in the matrix and finally α-Al/Al2Cu anomalous eutectic structure near the aluminum side. Gas pore entrapment and oxide film entrainment defect was detected within the interface next to the aluminum base metal.*

Keywords: *Bimetallic Components, Centrifugal Casting, Casting Defects, Interface, Rotational Speed.*

1. INTRODUCTION

Since its invention in 1809 [1], centrifugal casting method has been utilized both in horizontal and vertical modes. The horizontal configuration has been generally used to produce pipes, tubes, and cylinders etc. while the vertical orientation is generally used for short cylinders and rings [2].

Bimetallic structures are currently popular because of their combinational properties and economic advantages [3] even though the increased problems of recycling are starting to be realized, and may negate the apparent benefits of some examples. For instance, rolls can be produced via a two-sequence casting practice in which a wear or corrosion resistant alloy forms the outer surface while the bulk is made of a cheaper alloy [4]. In this case the mutual contamination of two iron-based alloys in the recycling process is not a significant problem.

Producing two or more layered casting components by centrifugal casting process has been a widely-used technique, and may become more important if the process can be understood and controlled. Diouf and Jones [5] point out that the quality of the interfacial bond depends on various factors, including substrate roughness, substrate coating, solidification mode etc. Additional important parameters include die rotation speed, cooling rate, substrate preheating temperature and pouring temperature. Whereas dual alloy rolls are typically cast in successive pours of two different alloys, allowing the first to substantially solidify prior to the pouring of the second, in this case the outer alloy is introduced into a cylindrical mold in solid form. The inner alloy is then poured in, reacting the surface of the solid outer alloy to form a variety of intermetallic phases.

Centrifugally cast parts appear to be less defective, in general, because of the directional nature of solidification [6-7]. However, despite this view, it has been suggested that surface turbulence during centrifugal casting is the most important, and usually neglected, source of many defects in parts produced by this casting method. The beneficial centrifugal action being mainly required to centrifuge out all of those defects which are introduced during the pouring stage. Thus, one may suggest that the aspects of the process are counter-productive [4].

The oxide films and inclusions, unfortunately introduced and/or formed during the pouring, can deleteriously affect the quality and reliability of centrifugally cast parts [8-9]. In general, it has been reported that near 80% of casting defects are formed from the air and gas entrapment in the melt during the pouring stage [4, 10-12]. It is expected that the centrifugal casting would not be much different.

The focus of this study is the characterization of various phases and an assessment of the various defects that form at the interface between the two alloys.

2. EXPERIMENTAL PROCEDURE

Chemical composition of $Cu_{65}Zn_{35}$ sheet and 99.8% pure aluminium used in this work are given in Tables 1 and 2. The formation of the brass cylinder, as a lining inside the solid mold, is shown in Fig. 1. Following the bending of the brass plate around a steel pipe using a rubber tool a piece of ceramic fiber paper was used to join the gap between the ends of the brass sheet. The inner surface of the brass rings was washed and cleaned using a mild soap detergent with warm water and a mild grinding were applied before pouring.

Two conditions with different liquid/solid volume ratios (VR) 1.5 and 2.5, of the alloys

Table 1. Chemical composition (wt.%) of CuZn35 sheet.

Material	Zn	Ni	Sn	Fe	Pb	Al	Cu
CuZn35	35	0.3	0.1	0.05	0.05	0.02	Bal.

Table 2. Chemical composition (wt.%) of the aluminum ingot.

Material	Si	Fe	Mg	Mn	Al
Al ingot	0.08	0.064	0.027	0.006	Bal.

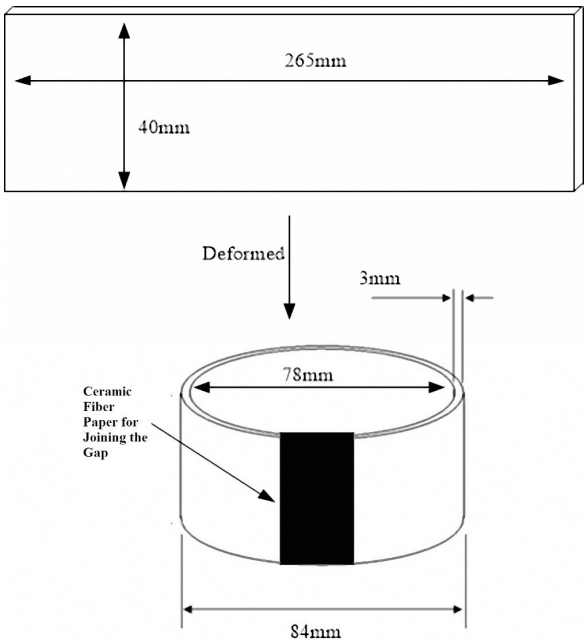

Fig. 1. Preparation process of the brass cylinders; brass sheets cut to 265×40×3 mm size and deformed to a cylindrical shape using asbestos and steel wire.

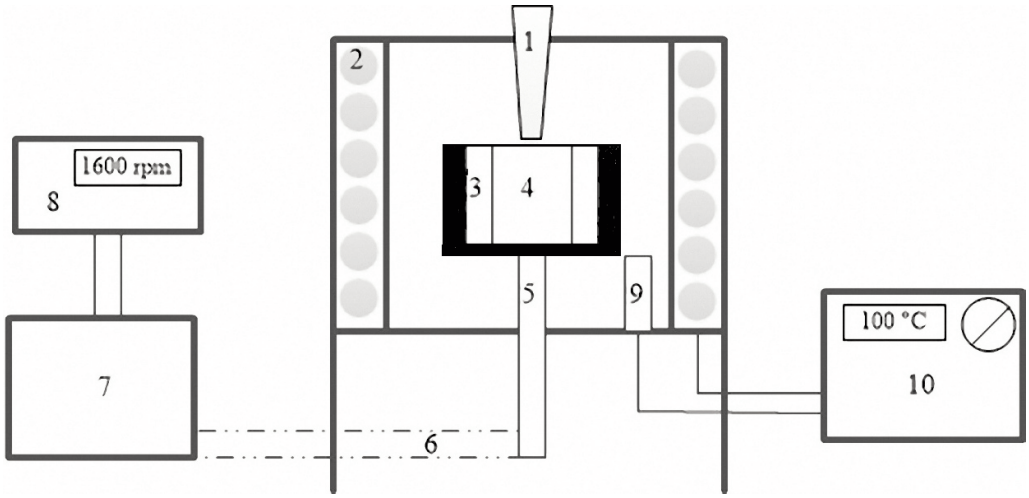

Fig. 2. Schematic representation of vertical centrifugal casting (VCC) machine, (1) sprue (2) heating element (3) brass cylinder (4) die cavity (5) spindle (6) belt pulley (7) electromotor (8) inverter (9) thermometer attached to the heating generator (10) heating generator and controller.

were used (the reader will notice that this volume ratio corresponds approximately to the thickness ratio of the two alloys at the instant of addition, prior to melting and reaction).

Commercial pure aluminum ingot, precisely cut and weighted (depend on liquid/solid VRs), was charged in a graphite crucible and melted by a resistance furnace. The prepared melt was then poured at 700°C into the Cu_65Zn_{35} hollow cylinder, preheated to 100 °C, and already spinning at its designated speed. The Vertical Centrifugal Casting (VCC) device consisted of a resistance-heated chamber, containing a spindle on which was attached a cast iron mold as a container lined with the brass sheet. The 'floor' of the cast iron container, which is impacted by the falling metal, is protected by an alumina wash. The preheated device was kept at 100 °C after pouring the aluminum melt and the resistance heater in the casting machine was not switched off, but continued to provide an environment near to 100 °C to the end of solidification of casting component after nearly 200 seconds

To investigate microstructural features, samples were cut from the castings as shown in Fig. 3. The samples were subjected to metallographic preparation using SiC papers and finally polishing with 0.3µm alumina powder. Olympus BX51M optical microscope (OM) and VEGA TESCAN scanning electron microscopy (SEM) were used to examine the microstructures. X-ray diffraction (XRD) was used to identify the

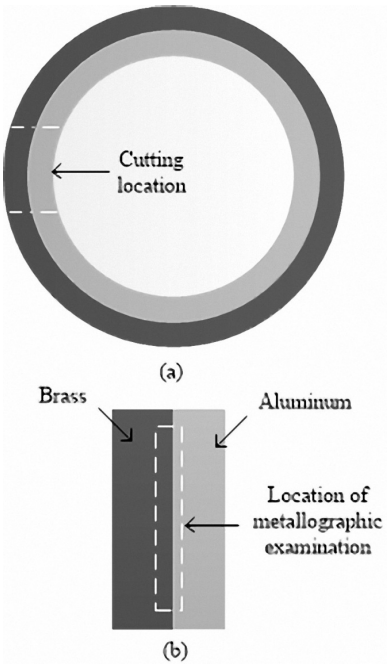

Fig. 3. Metallographic sample preparation steps, (a) cross section cutting, and (b) cutting to smaller dimension for metallographic observations.

precipitated phases. The angle range, the anode material, the characteristic Kα, the angular variation, and the experiment temperature were 20 to 80 degrees, copper, 1/54 A°, 0.05°, and 25°C, respectively. The results were extracted as intensity diagrams based on 2 theta.

3. RESULTS AND DISCUSSION

3. 1. Interface

The preparation condition and the resulting interfacial thickness are shown in Table 3. The formation of interfacial layer seems to be the result of a multi-component process in which the dissolution and reaction of the solid metal is provided by the heat content of the melt, the energy of formation of the intermetallics and multi-directional mechanical forces involved.

As shown in Fig. 4, increased rotational speed leads to the reduction of the thickness of reaction layer. This may be related to the increased cooling rate due to higher heat transfer by conduction across reduced air gap at the back of the brass sheet, now pressed more closely to the supporting container. A cross section of the interface of the sample 5 is shown in Fig. 5. Unbonded zones plus some pores near the interface are visible. Liu et al. [13], have suggested that presence of the surface oxide film on the solid is one of the main reasons resulting in the formation of the zones of poor metallurgical bonding at the interface. However, many researchers have gone further, citing the effect of the surface oxide film on both the solid and the melt surfaces [10, 12]. Despite attempts to reduce these problems, as described in the experimental method section, there is no doubt that oxide films on both the solid and liquid are present, and can affect the results of this work. The unbonded areas at the top and bottom of the bimetallic cylinder are structural defects which require to be solved by additional development work before industrial applications could be contemplated.

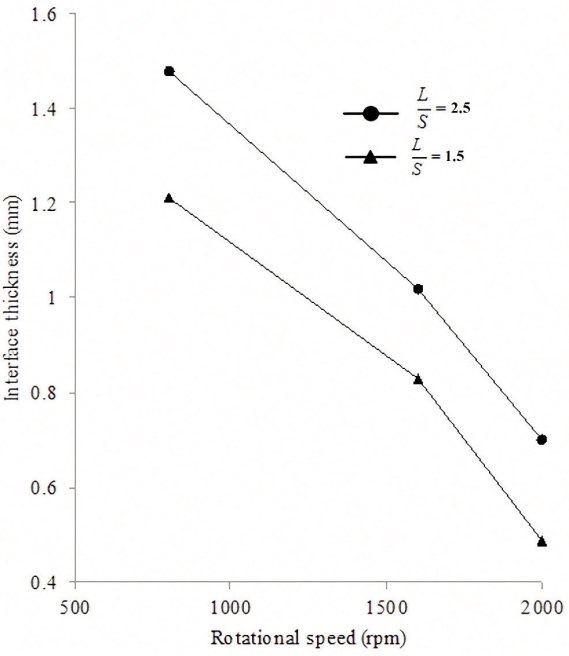

Fig. 4. Variation of the interfacial thickness versus increasing the rotational speeds (at 1.5 and 2.5 volume ratio and 100°C constant preheating temperature).

Table 3. The samples preparation conditions (pouring temperature, 700°C and brass cylinder preheating temperature, 100°C) and the resulted interfacial thickness.

Sample no.	Rotation per minute (rpm)	Liquid-to-solid VR (L/S)	Interfacial thickness (μm)
1	800	1.5	1210
2	1600	1.5	830
3	2000	1.5	490
4	800	2.5	1480
5	1600	2.5	1020
6	2000	2.5	700

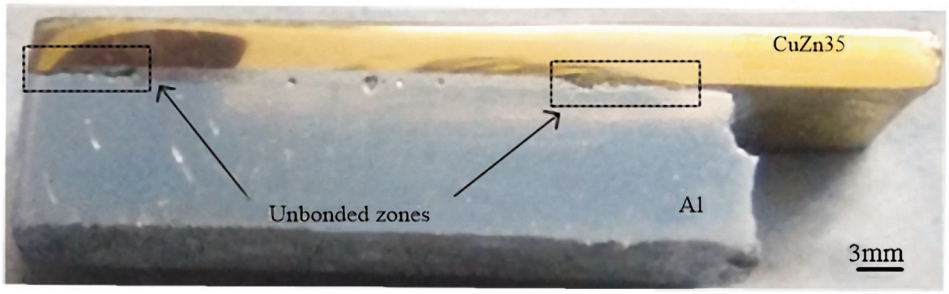

Fig. 5. Cross-sectional area of the sample 5 showing unbonded zones.

3. 2. Phase Characterization

SEM images of the sample 1, which are typical among six cast samples, are shown in Fig. 6. As can be observed in the EDS results (Table 4), the interface is composed of four discernible phases which have been formed and/or distributed in three zones shown in Fig. 6a.

Zone 1 in Fig. 6a, consists of two layers, $Al_2Cu_5Zn_4$ and Al_3Cu_3Zn, about 50 µm thick as shown in Fig. 6b, in which A2 ($Al_2Cu_5Zn_4$) is nearly 3 times thicker than A3 (Al_3Cu_3Zn). This two-layered zone is possibly the result of either fast dissolving of Zn and Cu, present in the solid brass, into the Al melt and/or diffusion of Al through Cu-Zn alloy during solidification. However, as one may expect, this two-layered zone is very brittle and breakage of the casting from such phase is expected as has been reported in other work [14].

The wave-like interface (Fig. 6b) is typical of a surface undergoing shear; waves, and especially breaking waves, are characteristic features of the shearing of two fluids, in this case

Table 4. EDS analysis results of the marked areas shown in Fig. 6b-d (Atomic %).

Point	Element composition (Atomic %)			Suggested compound
	Zn	Cu	Al	
A1	36.72	63.28	-	CuZn35
A2	36.94	45.08	17.99	$Al_2Cu_5Zn_4$
A3	14.23	41.8	43.98	Al_3Cu_3Zn
A4	1.47	25.35	73.18	Al_2Cu
A5	28.23	2.28	69.49	$Al_{0.7}Zn_{0.3}$
A6	0.99	25.38	74.62	Al_2Cu
A7	-	-	99.99	Al

two liquid layers, analogously to the phenomenon of the shearing action of wind over the seas. It confirms conditions known to be common in centrifugal casting, in which the cast metal only gradually accelerates up to the speed of the mold.

A detailed secondary electron micrograph of zone 2 is shown in Fig. 6c. There are some interesting features in this micrograph like indentation of some facets of the Al_2Cu phases. In some places, like the upper part of micrograph, Al_2Cu phase looks like a piece of stretched chocolate. This seems to be the result of multidirectional forces, acting on the Al_2Cu

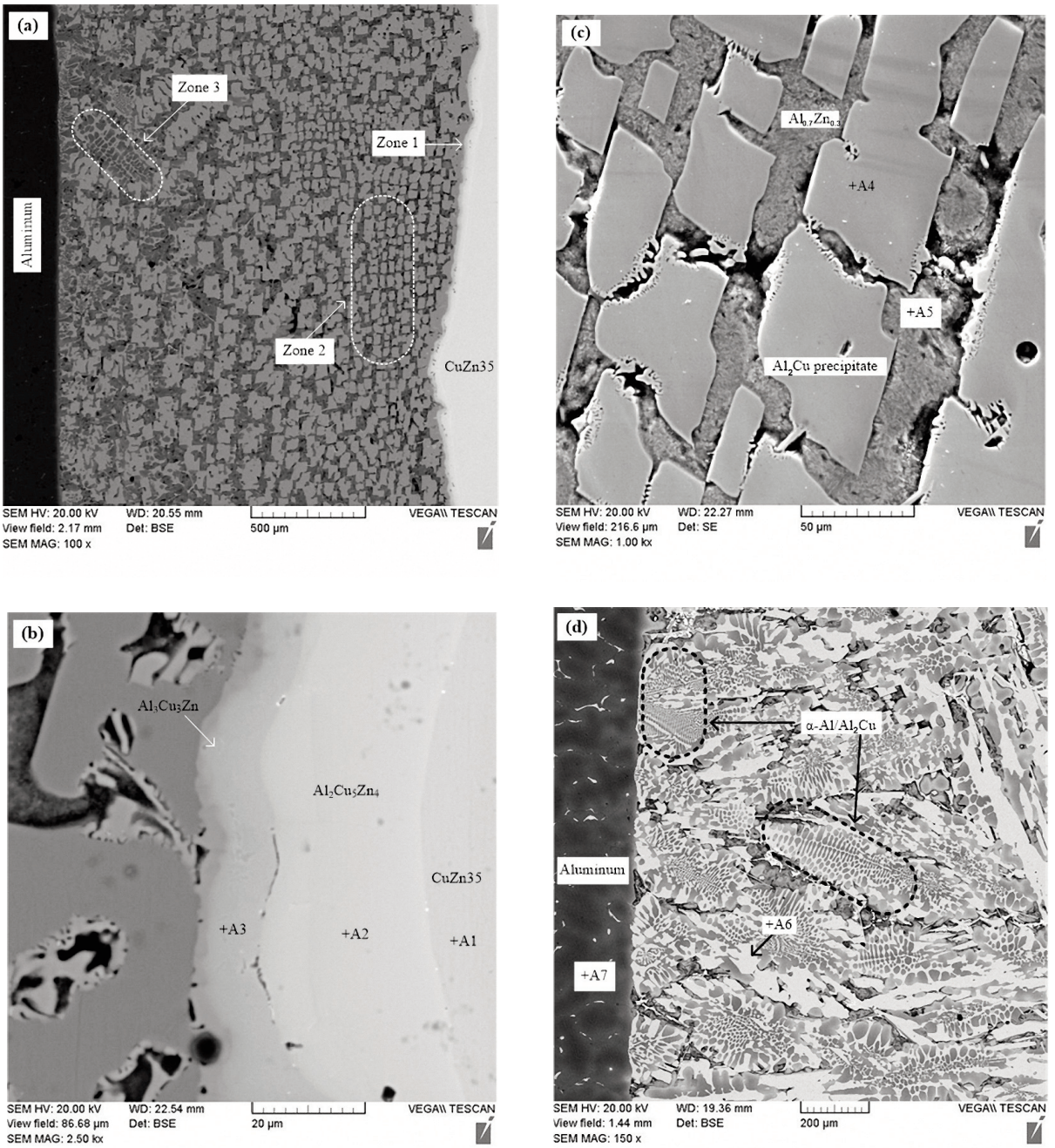

Fig. 6. SEM micrographs of (a) the interface of sample 1 showing three discrete zones, (b) higher magnification of zone 1, showing more details of the formed intermetallics, (c) higher magnification of zone 2 showing the shape and distribution condition of Al2Cu participates, and (d) showing the size and form of eutectic structure in zone 3.

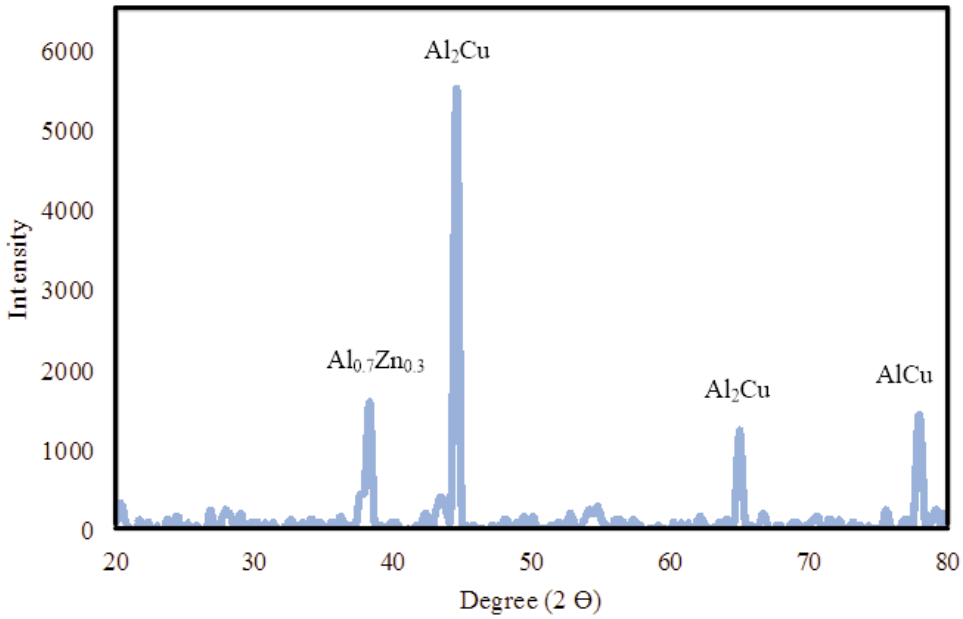

Fig. 7. XRD taken from the interface (zone 3).

phase during its formation and following solidification. (The Al-Cu phase diagram shows a numerous array of phases, and this situation will be further complicated by the presence of Zn) Finally α-Al/Al_2Cu eutectic structure near the aluminum side (labelled as Zone 3 in Fig. 6a) is visible.

The presence of dendrites of Al_2Cu (Fig. 6d) proves that the interface between the Al and brass did melt. The significant content of Al_2Cu (Fig. 6c) reflects the fact that this intermetallic is the most stable compound in the Al-Cu system. Its great stability gives it a high melting point, and will ensure a high release of latent heat when the alloy solidifies. XRD taken from the zone 3 is shown in Fig. 7 in which the main phases in this area are visible.

3. 3. Anomalous Eutectic Formation

When a melt is undercooled exceeding a critical undercooling, anomalous eutectic form with a completely different morphology compared to regular lamellar or rod eutectics, in some eutectic alloys [15]. Formation of anomalous eutectic is a common phenomenon in alloy systems, such as Ni–Sn [16-17], Ni–Sb [18], Co–Sn [19-20] and Ag–Cu [21-22]. Most of these alloys are binary systems of transition elements like Co, Ni, Cu, Ag and post-transition elements such as Sn, Sb, Ge and so on. The theoretical background for this type of microstructure has been discussed by Kurz et al. [23]. Although there have been many reports on anomalous eutectics, many explanations and controversies still exist regarding their formation mechanism. However, theoretical analyses indicate that, a transition from solutal-diffusion-controlled growth to thermal-diffusion-controlled growth at some undercooling situation may have the main contribution for the formation of this type of eutectic [24]. It seems the high speed of heat extraction during centrifugal process not only reduces the thickness of the interfacial zone (see Fig. 4) but also play a key role in the formation of anomalous eutectic. Interestingly, even the cooling effect of a brass core in the compound casting of Al/brass has created anomalous eutectic as is reported in another work [14].

3. 4. Defects (Pore and Crack)

Entrapped gas pores, at the interfacial zone of sample 3, are shown in Fig. 8a. According to this image these pores are very close to the aluminium side. It means the gas/air bubbles in

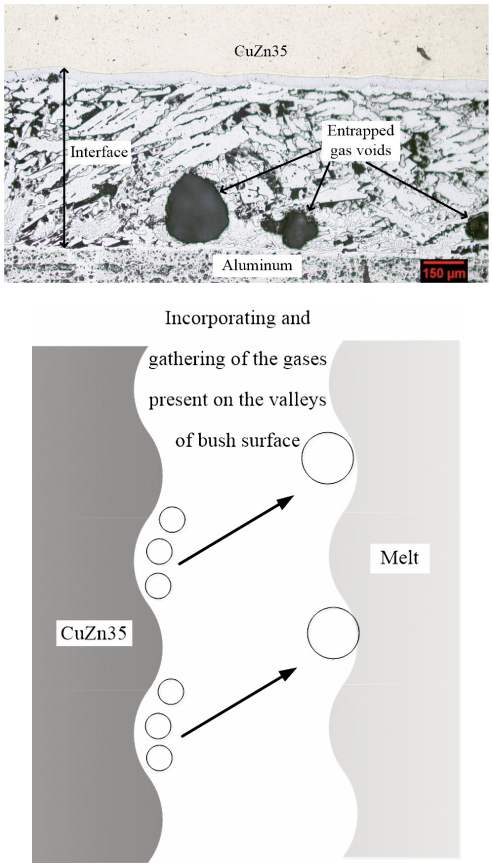

Fig. 8. Representative optical micrograph of the sample 3 showing entrapped gas voids at the interface, (b) Schematic representation of gas pores creation at the Al/CuZn35 interface.

the melt, probably because of the surface turbulence [25-26] and/or the air present at the micro valley of the solid ring, may expand and finally moves toward internal periphery and entrapped (Fig. 8b). It appears like these gas bubbles are hard up against a patch of a very thin alumina film created from the original impact of the liquid Al against the solid brass surface. Air would be expected to be trapped in places between the solid brass oxide and the solid alumina film on the liquid. The surface of the brass would melt, and entrapped air between the Al and the brass would be trapped inside the thickening layer of brass, unable to enter the liquid Al because of the alumina film, exactly as shown in Fig. 8a. If the alumina film had not been in place the bubbles would have been free to migrate through the liquid Al under the centrifugal action, and finally escape at the inner bore of the liquid metal (see also Fig. 5).

Fig. 9a shows an oxide film which is formed perpendicular to the cut section at Al/CuZn35 interface. In fact, surface oxide films folding over and entrapment into the melt may be located at any place in final casting structure creating a crack. These sort of casting defects has been reported by many researchers [4, 9, 11]. A typical crack, visible on the Fig. 9a, was opened up and

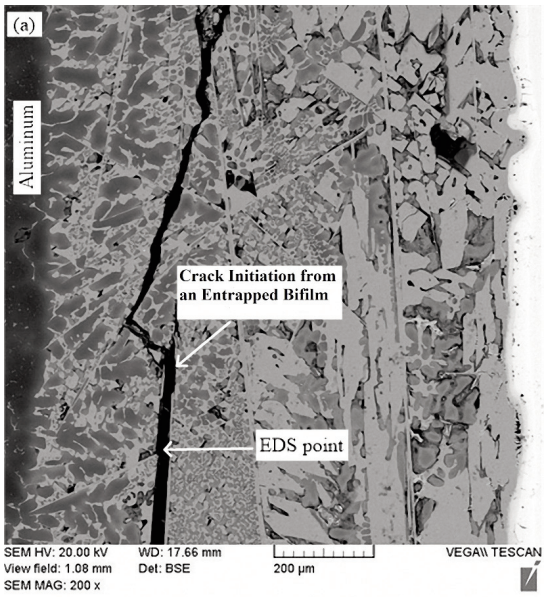

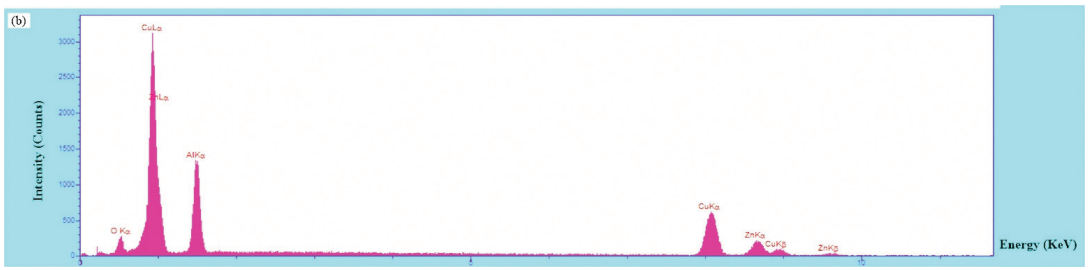

Fig. 9. (a) SEM micrograph showing a long crack and, (b) EDS spectra of the opened crack side view (showing oxide film acting as crack initiator)

EDX performed on the obtained surface as is shown on Fig. 9b. The presence of oxygen in this EDX is possibly related to the formation of surface oxide film during casting process. Many researchers [4, 9-12, 14, 27] has suggested that oxidized layers, between internal dry side of the entrapped bifilm, prevents contact between them so that no bonding can be established.

Intrinsic surface turbulence of this process increases aluminium oxide film breakages and leads to folding and engulfing them into the melt, according to Dai et al. [28]. For the future, better designs of pouring system might greatly reduce the bifilm population in the cast alloy, and therefore reduce and possibly eliminate the cracking problem. Pouring the melt onto the spinning surface to match the surface velocity would almost certainly be a great help, greatly reducing the shearing effects.

4. CONCLUSIONS

1. Interfacial layers of Al/Brass, from the solid brass side to Al side, are firstly two intermetallics $Al_2Cu_5Zn_4$, Al_3Cu_3Zn (Zone 1) and then Al2Cu, as major precipitates, dispersed in possibly an αAl/Al-Zn eutectic (Zone 2) and finally α-Al/Al2Cu anomalous eutectic structure near the aluminum side (Zone 3).
2. Increased rotational speed leads to the reduction of the reaction layer which may be related to the increased cooling rate due to higher heat transfer by conduction across reduced air gap at the back of the brass ring.
3. Gas entrapment and surface aluminium oxide film entraining into the melt may be localized at different parts of the final casting structure which can possibly be prevented by better pouring exercise.

ACKNOWLEDGMENT

I would like to express my deep and sincere gratitude to Professor John Campbell for his comments on this work and revising most part of the manuscript. Financial support of the deputy of research of the Iran University of Science and Technology (IUST) is also acknowledged.

REFERENCES

1. Pola, A., "Advanced Casting Methodologies: Centrifugal Casting", Compreh. Mat. Pro., 2014, 47-51.
2. Watanbe, Y., Watanbe, S., and Matsuura, K., "Nickel-aluminides/steel clad pipe fabricated by reactive centrifugal casting method from liquid aluminum and solid nickel", Met. and Mat. Trans. A, 2003, 35 (5), 1517-1524.
3. Xu, G., Luo, A. A., Chen, Y. and Sachdev, A. K., "Interfacial Phenomena in Magnesium /Aluminum Bi-metallic Castings", Materials Science&Engineering A, 2014, 595, 154-158.
4. Campbell, J., "Complete Casting Handbook", Butt.-Heinemann: University of Birmingham, UK, 2011, 979-985.
5. Diouf, P. and Jones, A. "Investigation of Bond Strength in Centrifugal Lining of Babbitt on Cast Iron". Metallurgical and Materials Transactions A, 2010, 41, 603-609.
6. Shailesh, R. A., Tattimani, M. S. and Rao, S. S., "Understanding Melt Flow Behavior for Al-Si Alloys Processed Through Vertical Centrifugal Casting" Materials and Manufacturing Processes, 2015, 30, 1305-1311.
7. Changyun, L., Haiyan, W., Shiping, W., Lei, X., Kuangfei, W. and Hengzhi, F., "Research on Mould Filling and Solidification of Titanium Alloy in Vertical Centrifugal Casting", Rare Metal Materials and Engineering, 2010, 39, 388-392.
8. Zhou, J. X., Shen, X., Yin, Y. J., Guo, Z. and Wang, H., "Gas-liquid Two Phase Flow Modelling of Incompressible Fluid and Experimental Validation Studies in Vertical Centrifugal Casting" IOP Conference Series: Materials Science and Engineering, 2015, 84.
9. Trejo, E. Centrifugal Casting of an Aluminium Alloy, Doctor of Phi. Thesis, University of Birmingham, 2011.
10. Divandari, M. and Campbell, J. "Oxide Film Characteristics of Al–7Si–Mg Alloy in Dynamic Conditions in Casting", International Journal of Cast Metals Research, 2004, 17(3), 182-187.
11. Reilly, C., Green, N. R. and Jolly, M. R. "Surface Oxide Film Entrainment Mechanisms in Shape Casting Running Systems" Metallurgical and Materials Transactions B,

2009, 40, 850-858.
12. Hajjari, E., Divandari, M., Razavi, S. H., Homma, T. and Kamado, S., "Microstructure Characteristics and Mechanical Properties of Al 413/Mg Joint in Compound Casting Process". Metallurgical and Materials Transactions A, 2012, 43, 4667-4677.
13. Liu, X. R., Cao, C. D. and Weisheng, B., "Microstructure Evolution and Solidification Kinetics of Undercooled Co–Ge Eutectic Alloys". Scripta Materialia, 2002, 46, 13–18.
14. Akbarifar, M., Divandari, M., Inter. J. of Metalcasting, 2016, doi:10.1007/s40962-016-0101-z
15. B. L. Jones Metall. Trans. 2:2950–1, (1971), doi: 101007/BF02813283
16. Kattamis, T. Z., and Flemings., M. C., "Structure of undercooled Ni-Sn eutectic", Metallurgical and Materials Transactions 1970, 1.5, 1449-1451.
17. Wu, Y., Piccone, T. J., Shiohara, Y. and Flemings, M. C., "Dendritic growth of undercooled nickel tin: Part III" Metallurgical Transactions A, 1988,19(4), 1109-1119.
18. Han, X. J., and B. Wei. "Microstructural characteristics of Ni-Sb eutectic alloys under substantial undercooling and containerless solidification conditions", Metallurgical and Materials Transactions A, 2002, 33(4), 1221-1228.
19. Liu, L., Li, J. F., and Zhou., Y. H., "Solidification interface morphology pattern in the undercooled Co–24.0 at. % Sn eutectic melt", Acta Materialia, 2011, 59(14), 5558-5567.
20. Liu, L., Wei, X. X., Huang, Q. S., Li, J. F., Cheng, X. H. and Zhou. Y. H., "Anomalous eutectic formation in the solidification of undercooled Co–Sn alloys" Journal of Crystal Growth, 2012, 358, 20-28.
21. Zhao, S., Li, J. F., Liu, L. and Zhou, Y. H., "Cellular growth of lamellar eutectics in undercooled Ag–Cu alloy", Materials Characterization, 2009, 60(6), 519-524.
22. Clopet, C. R., Cochrane, R. F. and Mullis, A. M., "The origin of anomalous eutectic structures in undercooled Ag–Cu alloy", Acta Materialia, 2013, 61(18), 6894-6902.
23. Kurz, W., Giovanola, B. and Trivedi, R., "Theory of microstructural development during rapid solidification", Acta Metallurgica, 1986, 34(5), 823-830.
24. Wen-Jing, Y. and Bing-Bo, W., Microstructural evolution during containerless rapid solidification of Co-Si alloys. Chinese Physics, 2003, 12(11), 1272.
25. Divandari, M. and Campbell, J., "Mechanisms of bubble trail formation in castings", Trans. AFS, 2001, 109, 433-442.
26. Habibollahzadeh, A., Campbell, J., Trans. AFS, 2003, 111, No 03-021 P 675-684,
27. Aryafar, M., Raiszadeh, R. and Shalbafzadeh, A., "Healing of double oxide film defects in A356 aluminium melt", Journal of materials science, 2010, 45(11), 3041-3051.
28. Dai, X., Jolly, M. R., Yang, X. and Campbell, J. "Modelling of Liquid Metal Flow and Oxide Film Defects in Filling of Aluminium Alloy Castings", Materials Science and Engineering, 2012, 33.